

# Effects of Mn on Corrosion Resistant Property of AZ91 Alloys

Li Xiaoyan<sup>1,2</sup>, Li Mingzhao<sup>1,2</sup>, Fan Liuqun<sup>1,2</sup>, Wang Haiyan<sup>1,2</sup>, Feng Chong<sup>1,2</sup>, Meng Hua<sup>2</sup>

<sup>1</sup> Taiyuan University of Technology, Taiyuan 030024, China; <sup>2</sup> Key Laboratory of Interface Science and Engineering in Advanced Materials, Ministry of Education, Taiyuan 030024, China

**Abstract:** The effect of Mn on the corrosion resistant property of heat-treated AZ91 alloys was investigated by electrochemical, static mass loss tests and salt spray corrosion method. The micromorphologies of the corroded samples of the alloys were studied by scanning electron microscope (SEM), and the phase composition and the corrosion products of the alloys were analyzed by X-ray diffractometer (XRD). Results demonstrate that an independent phase Al<sub>6</sub>Mn is formed in AZ91 alloy. The solubility of the phase in solid solution of Mg can increase the electrode potential of Mg. Mn addition can increase the corrosion potential, decrease the corrosion current density of AZ91 alloys and reduce corrosion rates. Therefore, the corrosion resistance of alloys is improved. AZ91-0.8Mn alloy shows the best corrosion resistance capacity among all of the specimens among all of the specimens.

**Key words:** Mn; AZ91 alloy; corrosion resistance property

AZ91 alloy has much attractive advantages such as low density, high specific strength and excellent castability, but its bad corrosion behavior becomes a serious limitation to its widespread applications around the industries<sup>[1-4]</sup>. Many researches have found that the addition of adequate alloying elements can play an important role in improving its relevant corrosion property of magnesium and magnesium alloys. By now, only a few studies have been reported about the stress-corrosion cracking susceptibility of magnesium alloy after varied heat-treatment<sup>[5,6]</sup>, results show that the corrosion resistance is improved and the corrosion current density decreases in a 3.5 wt% NaCl solution after artificial aging at 260 °C for 4 h. However, so far no systematic research has been carried out on the effects of Mn addition on the corrosion resistance of heat-treated AZ91 alloys.

The present investigation was concentrated on studying the effect of Mn on corrosion behavior of AZ91 alloys prepared by heat treatment route to understand the role of Mn addition in the microstructures during the corrosion processes, includ-

ing electrochemical, and static weight loss tests, salt spray corrosion method and surface morphology.

## 1 Experiment

The starting materials were Al, Zn, Mg and Al-Mn master alloy. The experiment was divided into 4 groups with 0 wt% Mn, 0.4 wt% Mn, 0.8 wt% Mn and 1.2 wt% Mn, respectively. The chemicals compositions are shown in Table 1.

The alloys were prepared under the conditions of vacuum melting and argon protecting. The specimens with the addition of different amounts of Mn were cut into the cubes with the

**Table 1** AZ91-xMn alloy before and after melting (wt%)

Alloy	Before melting				After melting			
	Al	Zn	Mn	Mg	Al	Zn	Mn	Mg
AZ91	9.0	1.0	0	Bal	8.87	0.71	0	Bal.
AZ91-0.4Mn	9.0	1.0	0.4	Bal	8.89	0.72	0.39	Bal.
AZ91-0.8Mn	9.0	1.0	0.8	Bal	8.87	0.70	0.78	Bal.
AZ91-1.2Mn	9.0	1.0	1.2	Bal	8.88	0.71	1.18	Bal.

Received date: March 04, 2013

Foundation item: Project Implementation Supported by Shan Xi's Patent (121004); Metallurgical Engineering Characteristic Professional Construction Project  
Corresponding author: Li Mingzhao, Professor, College of Materials Science and Engineering, Taiyuan University of Technology, Taiyuan 030024, P. R. China, Tel: 0086-351-6010311, E-mail: limingzhaoty@126.com

Copyright © 2014, Northwest Institute for Nonferrous Metal Research. Published by Elsevier BV. All rights reserved.

sizes of 10 mm×10 mm×10 mm for the electrochemical experiment, the specimen sizes of static mass loss test and salt spray corrosion were 10 mm×10 mm×7 mm. The specimens were treated at 415 °C for 16, 20, 24 and 28 h<sup>[7]</sup> followed by quenching, then aged at 170 °C for 24 h. All the specimens were progressively polished by six finer grades of emery papers, the levels of which were 360#→600#→800#→1000#→1200#→2000#. The specimens were cleaned by acetone and ethanol.

Electrochemical polarization experiments were carried out using the PS-168 Corrosion Measurement System. Before electrochemical testing, the working surfaces of the samples were exposed to the solution of 3.5 wt% NaCl<sup>[8]</sup> at the temperature of (25±1) °C. The scanning area of the polarization voltage was set in the range of -2000 mV to 2000 mV coupled with the scanning rate set at 4 mV·s<sup>-1</sup>.

The polished samples were suspended in the solution of 3.5 wt% NaCl at the temperature of 20 °C for 8, 24, 48 and 144 h in static mass loss test<sup>[9]</sup>. Then the treated samples were immersed in 15% chromic acid solution for 10min to eliminate surface corrosive products. After that the samples would be cleaned by tap water and dried by blower<sup>[10]</sup>. Three times of parallel tests were carried out and average corrosion rates can be weighed by optical balance.

Salt fog experiments were conducted in the S991-013 salt fog corrosion experimental chamber, the inner temperature of which was (35±2) °C with the density of compressive air 1 kg·cm<sup>-2</sup> and the average spray distribution of 1~2 mL, 80 cm<sup>-2</sup>·h<sup>-1</sup>. The polished samples were placed in the corrosion experimental chamber for different time, e.g. of 4, 8, 12, 24 h and the corrosion solution was 5% NaCl solution. Three times of parallel tests were carried out and the average value was obtained.

The corrosion morphologies of samples were observed by JSU-6700F scanning electron microscope while Y-2000 automated X-ray diffractometer system was used to analyse corrosion products.

## 2 Discussion

### 2.1 Electrochemical corrosion

The electrochemical corrosion behavior of the samples tested in 3.5% NaCl solution is shown in Fig.1. All the samples do not show any clear passivity in this solution. The values of the corrosion current density and corrosion potential for each polarization curve are listed in Table 2. It is clear to see that Mn addition makes the polarization curve move toward more positive direction, the anodic reaction is blocked. Compared with the pure AZ91 alloy, more corrosion potential values and less corrosion current density values were obtained. According to Faraday's law, the current density is proportional to the corrosion rate, therefore, we can come to the conclusion that the addition of Mn can improve the corrosion resistance of AZ91 alloys by decreasing the alloy current density. How-

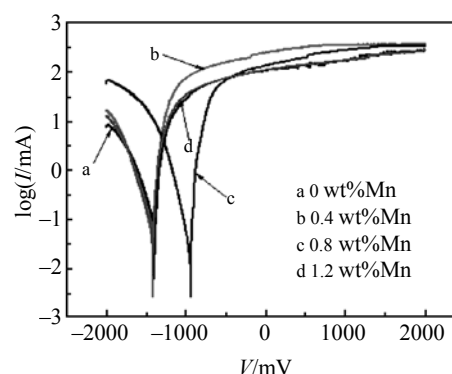


Fig.1 Effect of Mn on the polarization curves of heat-treated AZ91-xMn alloys

Table 2 Corrosion potential and current of heat-treated AZ91-xMn alloys

Alloy	Current density/mA·cm <sup>-2</sup>	Potential/mV
AZ91	0.098	-1407
AZ91-0.4Mn	0.034	-1415
AZ91-0.8Mn	0.023	-949
AZ91-1.2Mn	0.073	-1394

ever, while the content of Mn exceeds certain amount, the polarization curve begins to shift to the opposite and the corrosion resistance of AZ91 will decline. It should be especially pointed out that the alloy with 0.8% Mn shows the least current density value which decreases by 76.5% compared with pure the AZ91 alloy. So alloy AZ91-0.8 Mn shows the best corrosion resistance capacity among all the specimens.

### 2.2 Static mass loss test

Fig.2 represents the relations between the corrosion rates and the corrosion time of AZ91-xMn alloy surfaces. As can be seen, the corrosion rates do not always show rising trend, firstly increases and then decrease. The corrosion is much lower than that of pure AZ91. It can be found out that the average corrosion rates decrease with increasing of Mn content, and AZ91-0.8Mn shows the lowest corrosion rate. Referring to Fig.1, the deterioration in the corrosion resistance on adding 1.2 wt% Mn is thought to be due to the microgalvanic effect. The morphologies of the surfaces of the heat-treated AZ91-xMn alloys after mass loss test for 24 h are displayed in Fig.3. The depths of corrosion pits presented in 0.4 wt% Mn AZ91 is much smaller than that in pure AZ91. AZ91-1.2Mn is corroded with its surface overlaid by an amount of corrosion products, but AZ91-0.8Mn is slightly corroded.

### 2.3 Salt spray corrosion

Fig.4 represents the surface morphologies of heat-treated AZ91-xMn alloys after salt spray test for 24 h. It is found that pure AZ91 is seriously corroded with its surface overlaid by an enormous amount of corrosion products and crystalline salt of sodium, but the alloys with Mn addition is less corroded, especially for alloy AZ91-0.8Mn. After removing the corrosion

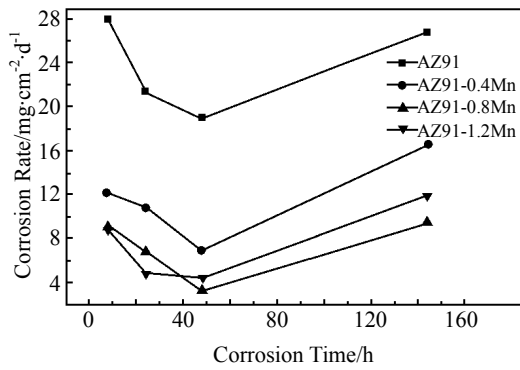


Fig.2 Relations between corrosion rates and corrosion time of AZ91-xMn alloys surface

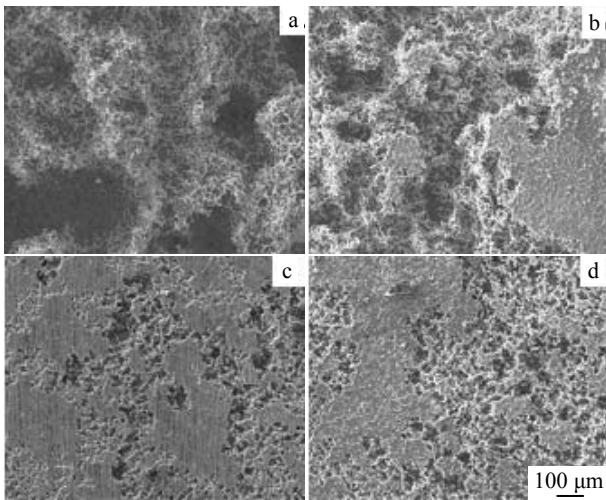


Fig.3 Surface morphologies of heat-treated AZ91-xMn alloys after mass loss test for 24 h: (a) without Mn, (b) 0.4 wt% Mn, (c) 0.8 wt% Mn, and (d) 1.2 wt% Mn

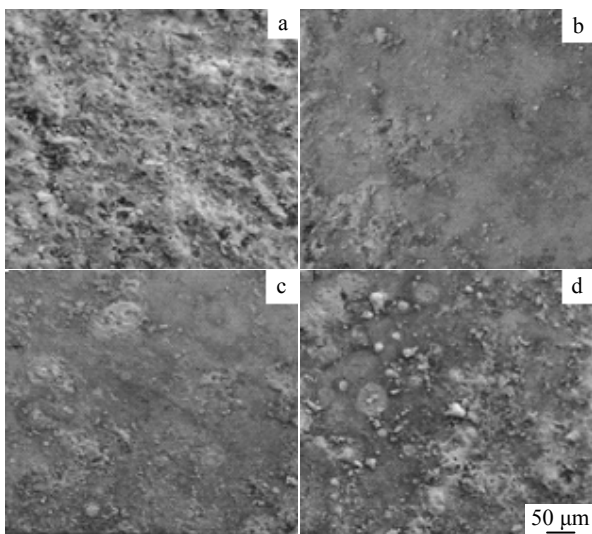


Fig.4 Surface morphologies of heat-treated AZ91-xMn alloys after salt spray test for 24 h: (a) without Mn, (b) 0.4 wt% Mn, (c) 0.8 wt% Mn, and (d) 1.2 wt% Mn

product, it can be clearly found that pure AZ91 alloy is corroded unevenly and displays large and deep corrosion pits. On the other hand, alloys AZ91-(0.4~1.2)Mn present an uniform corrosion and the corrosion pits are much smaller, especially for alloy AZ91-0.8 Mn. From the results it can be concluded that 0.8% Mn addition distinctly improve the corrosion resistance, but further Mn addition will increase the corrosion rate.

**2.4 Corrosion products analysis**

To get a clear understanding of the corrosion performance of Mn on AZ91 alloys, the corrosion products of pure AZ91 and AZ91-0.8 Mn were analyzed by XRD. XRD of the products of the electrochemical corrosion and static mass loss test are shown in Fig.5 and Fig.6, respectively. As it can be seen, the corrosion products are mainly Mg(OH)<sub>2</sub> and MgO according to the PDF card. Early corrosion product is MgO which is converted to Mg(OH)<sub>2</sub> because of instability<sup>[11]</sup>. The products of salt spray corrosion are displayed in Fig.7. The corrosion products are main Mg(OH)<sub>2</sub>, MgO and Mg<sub>17</sub>Al<sub>12</sub>. As to Mg<sub>17</sub>Al<sub>12</sub>, it is because α-Mg matrix around β phase is corroded and β phase has no place to attach<sup>[12]</sup>. Compared with the three corrosion products of XRD, no Mn compounds are found, it can be concluded that Mn addition can improve the AZ91 alloys corrosion resistance

**2.5 Corrosion mechanism analysis**

AZ91-xMn alloys were analysed by XRD in Fig.8 for further understanding of Mn on AZ91 alloy. α-Mg, β-Mg<sub>17</sub>Al<sub>12</sub> and a new phase Al<sub>6</sub>Mn exist in AZ91-xMn alloys. The crystal structure of α-Mg solid solution is the same as pure Mg, but β-Mg<sub>17</sub>Al<sub>12</sub> and Al<sub>6</sub>Mn are distributed mainly on grain boundary.

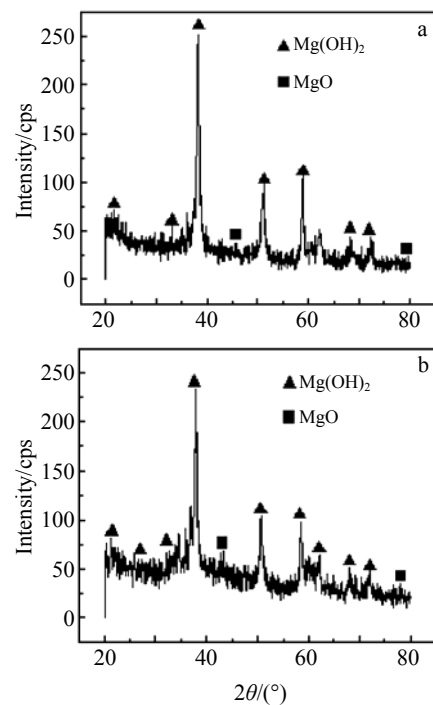


Fig.5 XRD patterns of the products of electrochemical corrosion: (a) AZ91 and (b) AZ91-0.8 Mn

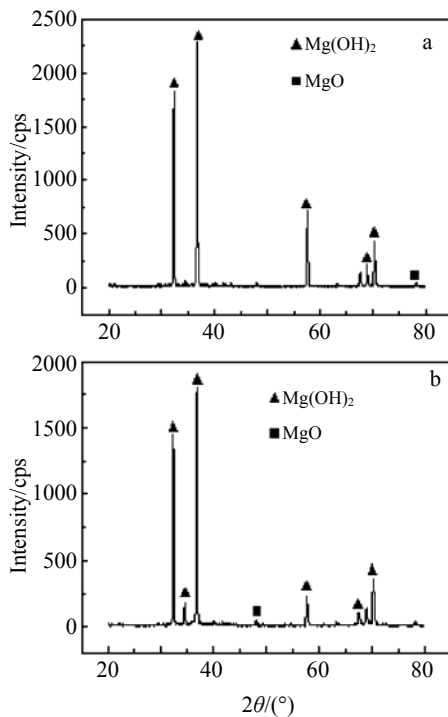


Fig.6 XRD patterns of the products of mass loss corrosion: (a) AZ91 and (b) AZ91-0.8 Mn

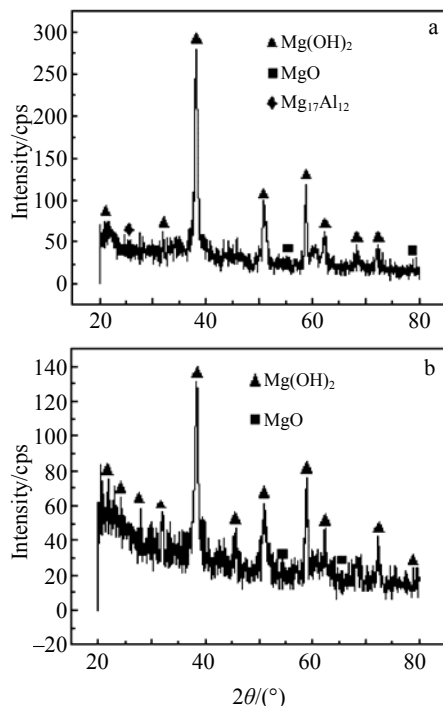


Fig.7 XRD patterns of the products of the salt spray test: (a) AZ91 and (b) AZ91-0.8 Mn

The reasons of Mn addition improving of the AZ91 alloys corrosion are as follows:

(1) Influence of corrosion potential

Mn addition will bring the formation of the formed

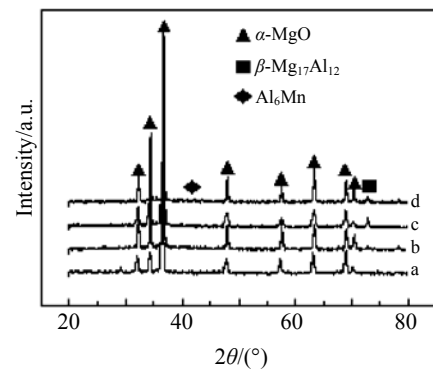


Fig.8 XRD patterns of AZ91-xMn alloys after heat-treated: (a) without Mn, (b) 0.4 wt% Mn, (c) 0.8 wt% Mn, and (d) 1.2 wt% Mn

independent phases such as  $Mg_4Mn$ ,  $Al_2Mn$ ,  $Al_6Mn$  with Mg and Al in AZ91 alloys on the basis of Mg-Mn binary phase diagram<sup>[13]</sup>. However, only  $Al_6Mn$  is detected in this experiment while other phases are inadequate to be found. According to corrosion parameters of the fact that once  $Al_6Mn$  dissolves in Mg solid solution, electrode potential of Mg is improved and then corrosion resistance of AZ91 alloys is enhanced.

(2) Function of Mn

Mn addition can improve distribution shape of the secondary phase. The smaller the grain size, the more the  $\beta$  phase It presents a continuous network dispersedly and uniformly.  $\beta$  phase and corrosion products act as corrosion barrier leading to the decrease of corrosion rates. It can be concluded an independent phase  $Al_6Mn$ , which not only reduces segregation of Al but also functions as a corrosion barrier, is formed by Mn and Al in AZ91<sup>[14]</sup>. Therefore, the corrosion rates of the alloys are decreased.

3 Conclusions

1) An independent phase  $Al_6Mn$ , which not only reduces segregation of Al but also functions as a corrosion barrier, is formed by Mn and Al in AZ91. Therefore, the corrosion rates of alloys are decreased.

2) Mn addition can increase the corrosion potential and decreased the corrosion current density of AZ91 alloys and the corrosion rates.

3) Electrochemical , static mass loss test and salt spray corrosion method show the same results, that is, alloy AZ91-0.8 Mn exhibit the best corrosion resistance capacity.

References

- 1 Pan Fusheng, Yang Mingbo. *Transactions of Nonferrous Metals Society of China*[J], 2011, 21: 2382
- 2 Cheng Renju, Pan Fusheng, Yang Mingbo. *Journal of University of Science and Technology Beijing*[J], 2008, 30: 1397 (in Chinese)

- 3 Ding Wenjiang, Zeng Xiaoqin. *Acta Metallurgica Sinica*[J], 2010, 46: 1450
- 4 Zhang Xinming, Xiao Yang, Chen Jianmei et al. *Transactions of Nonferrous Metals Society of China*[J], 2006, 16: 518
- 5 Fujii K, Kawabata T, Matsuda K et al. *Materials Science Forum*[J], 2007, 561: 311
- 6 Tsao L C. *International Journal of Materials Research*[J], 2010, 101: 9
- 7 Miura Kazuma, Kobayashi Yasunori, Naito Takayuki et al. *Journal of the Japan Institute of Metals*[J], 2010, 74: 771
- 8 Shang Wei, Shi Xichang. *Chinese Journal of Materials Research*[J], 2011, 25: 58 (in Chinese)
- 9 Song D H, Lee C W, Nam K Y et al. *Mater Sci Forum*[J], 2007, 539: 1784
- 10 Wan Xiaofeng, Sun Yangshan, Xue Feng et al. *Rare Metal Materials and Engineering*[J], 2010, 39(11): 2112 (in Chinese)
- 11 Rajan Ambat, Naing Aung, Zhou W. *Corrosion Science*[J], 2000, 42: 1433
- 12 Cao Chunan. *Principle of Electrochemical Corrosion*[M]. Beijing: Chemical Industry Press, 2004 (in Chinese)
- 13 Liu Ansheng. *Diagrams of Binary Alloys State*[M]. Beijing: Metallurgical Industry Press, 2004 (in Chinese)
- 14 Xia Lanting, Gao Shan, Luo Xiaoping et al. *Foundry*[J], 2005, 54: 794

## Mn 对 AZ91 合金耐腐蚀性能的影响

李晓艳<sup>1,2</sup>, 李明照<sup>1,2</sup>, 范刘群<sup>1,2</sup>, 王海燕<sup>1,2</sup>, 冯冲<sup>1,2</sup>, 孟华<sup>2</sup>

(1. 太原理工大学, 山西 太原 030024)

(2. 教育部新材料界面与工程重点实验室, 山西 太原 030024)

**摘要:** 采用电化学、静态失重、盐雾腐蚀法研究了 Mn 对热处理态 AZ91 合金耐蚀性能的影响, 利用扫描电镜观察试样的微观形貌, 用 X 射线衍射仪分析合金的物相组成和腐蚀产物。结果表明, Mn 与 AZ91 合金中的 Al 形成了独立相 Al<sub>6</sub>Mn, 该相溶解到 Mg 固溶体中提高了 Mg 的电极电位, 进而提高了合金的耐腐蚀性; Mn 加入后使合金的自腐蚀电位升高, 自腐蚀电流密度降低, 降低了合金的腐蚀速率, 进而提高了合金的耐腐蚀性能, 且三种实验方法都表明 AZ91-0.8Mn 合金的耐腐蚀性能最好。

**关键词:** Mn; AZ91 合金; 耐腐蚀性能

---

作者简介: 李晓艳, 女, 1986 年生, 硕士生, 太原理工大学材料科学与工程学院, 山西 太原 030024, 电话: 0351-6010311, E-mail: lixiaoyan87@sina.cn